Neural coding of action in 3 dimensions: Task- and time-invariant reference frames for visuospatial and motor-related activity in parietal area V6A

Hadjidimitrakis K.[1,2°],Ghodrati M. [2,3°], Breveglieri R.[1] Rosa M.G.P. [2,3*] Fattori P.[1*]

[1] Department of Biomedical and Neuromotor Sciences, University of Bologna, Piazza di Porta San Donato 2, Bologna 40126, Italy.

[2] Department of Physiology and Biomedicine Discovery Institute, Monash University, Clayton, VIC 3800, Australia

[3] ARC Centre of Excellence for Integrative Brain function, Monash University, Clayton, VIC 3800, Australia.

Running title: Arm and target integration in depth

Correspondence: Dr Kostas Hadjidimitrakis,

Department of Biomedical and Neuromotor Sciences,

University of Bologna, Piazza di Porta San Donato 2,

Bologna 40126, Italy E-mail: kon.chatzidimitrakis@unibo.it

° Equal first authors

* Equal last authors

Abstract

Goal-directed movements involve a series of neural computations that compare the sensory representations of goal location and effector position, and transform these into motor commands. Neurons in posterior parietal cortex (PPC) control several effectors (e.g. eye, hand, foot) and encode goal location in a variety of spatial coordinate systems, including those anchored to gaze direction, and to the positions of the head, shoulder or hand. However, there is little evidence on whether reference frames depend also on the effector and/or type of motor response. We addressed this issue in macaque PPC area V6A, where previous reports using a fixate-to-reach in depth task, from different starting arm positions, indicated that most units use mixed body/hand-centered coordinates. Here, we applied singular value decomposition and gradient analyses to characterize the reference frames in V6A while the animals, instead of arm reaching, performed a non-spatial motor response (hand lift). We found that most neurons used mixed body/hand coordinates, instead of "pure" body-, or hand-centered coordinates. During the task progress the effect of hand position on activity became stronger compared to target location. Activity consistent with body-centered coding was present only in a subset of neurons active early in the task. Applying the same analyses to a population of V6A neurons recorded during the fixate-to-reach task yielded similar results. These findings suggest that V6A neurons use consistent reference frames between spatial and non-spatial motor responses, a functional property that may allow the integration of spatial awareness and movement control.

Keywords: posterior parietal cortex, depth, reach**,** reference frame, visuomotor transformation

Introduction

During goal-directed behavior, **neurons in parietal and frontal cortex** encode spatial information in a variety of frames of reference, including eye-centered, hand-centered, and body/head-centered. There are also neurons showing mixed frames of reference (i.e. the neuron's response during movement to a given spatial location is modulated by the position of several body parts simultaneously (Buneo et al. 2002, 2008; Pesaran et al., 2006, 2010; Batista et al. 2007; Marzocchi et al., 2008; Mullette-Gillman et al., 2005; 2009; Bremner and Andersen, 2012). Recently, mixed frames of reference (also referred to as intermediate or hybrid) have emerged as the most prevalent type in numerous neurophysiological studies, which used various tasks and sensory inputs (Mullette-Gillman et al. 2005, 2009; Chang and Snyder 2010; McGuire and Sabes 2011; Hadjidimitrakis et al 2014a, 2017; Bosco et al. 2015; 2016; Sajad et al. 2016; Piserchia et al. 2017; Chen et al. 2018). Computational work suggested that mixed representations could be important for the nonlinear computations performed during reference frame transformations in 3D space (Pouget and Snyder 2000), and that they emerge naturally in neural networks performing such transformations (Blohm 2012). Furthermore, they could be beneficial for the flexibility of reference frames, not only during the temporal evolution from a sensory to motor phase occurring within a single task, but also when task demands (i.e. type of sensory input or motor response) are different.

The flexibility of reference frames across different tasks has been mainly tested by changing the modality of sensory input regarding target location. In these studies, the spatial representations were compared during reaching or grasping movements towards visual and proprioceptive targets (Bernier and Grafton 2010; McGuire and Sabes 2011; Leone et al. 2015) and during saccades towards visual or auditory targets (Mullette-Gillman et al. 2005, 2009). Significant changes in reference frames were reported in some parietal and frontal areas

(Bernier and Grafton 2010; Leone et al. 2015), whereas in other regions, the majority of cells showed stable reference frames (Mullette-Gillman et al. 2005, 2009; Buneo et al. 2008; McGuire and Sabes 2011; Hadjidimitrakis et al. 2017).

Compared to the effects of sensory modality, little is known about the influence of the motor response on the reference frames. This seems rather striking given the numerous studies investigating effector specificity in the parietal and frontal cortex. To our knowledge, only Pesaran and colleagues (2010) compared the reference frames of reach- and saccade-related activity in dorsal premotor cortex (PMd), using reaches and saccades performed from various initial eye and hand positions towards targets presented at fixed distance from the animals. According to this study, during saccades the spatial tuning of PMd cells tended to be modulated solely by either the eye or the hand position, or encoded the hand position with respect to the eye. Differently, during reaches, most neurons showed mixed sensitivity to these frames (Pesaran et al. 2006; 2010). This finding suggested that the effector could have some effect on the spatial representations. However, since both reaches and saccades are spatially targeted motor responses, it is unknown how the spatial representations adjust in behavioural contexts where there is no requirement for a target-oriented motor response, or when a non-spatial stereotyped motor response (i.e. button press and release) is performed. In PMd, the "Go" cue location was reported to affect the activity of some neurons even when the animals always responded with the same non-spatial motor response (Boussaoud & Wise, 1993; di Pellegrino & Wise, 1993). However, there are no relevant studies in the posterior parietal cortex (PPC) despite the fact that strong visuospatial activity has been reported (Battaglia-Mayer et al. 2001; Heider et al. 2010; Hadjidimitrakis et al. 2011; 2012).

In the present study, we addressed this issue in PPC area V6A, which processes both visuospatial and reach-related signals (Breveglieri et al 2012; 2014). We recorded V6A activity while monkeys fixated visual targets at various locations in 3D space and, after the Go cue,

performed a non-spatial motor response (lifting their hand from a button). In this task we varied the resting position of the hand between two locations at the near and far peripersonal space, and studied the body- and hand-centered reference frames across the task progress. We then compared findings with another population of V6A cells recorded in the same experimental setup while reaching movements were performed. If the reference frames are similar, this would suggest that V6A activity reflects a default reach plan. Alternatively, visuospatial activity might be linked to other processes (i.e. attentional) unrelated to movement planning.

Materials and Methods

General procedures. Two male macaque monkeys (*Macaca fascicularis*) weighing 4.4 Kg and 6 Kg were used. Initially, the animals were habituated to sit in a primate chair and interact with the experimenters. Then, a head restraint system and a recording chamber were surgically implanted under general anesthesia (sodium thiopenthal, 8mg/kg.h, i.v.) following the procedures reported by Galletti et al. (1995). A full program of postoperative analgesia (ketorolac trometazyn, 1mg/kg i.m. immediately after surgery, and 1.6 mg/kg i.m. on the following days) and antibiotic care (Ritardomicina, benzathine benzylpenicillin + dihydrostreptomycin + streptomycin, 1-1.4 ml/10kg every 5-6 days) followed surgery. Experiments were performed in accordance with national laws on care and use of laboratory animals and with the European Communities Council Directive of November 24, 1986 (86/609/EEC) and that of 22th September 2010 (2010/63/EU). All the experimental protocols were approved by the Bioethical Committee of the University of Bologna. Training and recording sessions were not carried out if the animals showed any behavioral and clinical sign of pain or distress.

Extracellular recording techniques and procedures to reconstruct microelectrode penetrations were similar to those described in other reports (e.g. Galletti et al. 1996). Single cell activity was extracellularly recorded from the anterior bank of the parieto-occipital sulcus. Area V6A was initially recognized on functional grounds following the criteria described in Galletti et al. (1999), and later confirmed following the cytoarchitectonic criteria according to Luppino et al. (2005). We performed multiple electrode penetrations using a five-channel multielectrode recording system (Thomas Recording). The electrode signals were amplified (at a gain of 10,000x) and filtered (bandpass between 0.5 and 5 kHz). Action potentials in each channel were isolated with a waveform discriminator (Multi Spike Detector; Alpha Omega Engineering) and were sampled at 100 kHz.

Recording locations. Histological reconstructions have been performed following the procedures detailed in previous publications (Galletti et al. 1999; Fillipini et al. 2018; Gamberini et al. 2018). Briefly, electrode tracks and the approximate location of each recording site were reconstructed on histological sections of the brain on the basis of electrolytic lesions and several other cues, such as the coordinates of penetrations within recording chamber, the kind of cortical areas passed through before reaching the region of interest, the depths of passage points between gray and white matter. All neurons of the present work were assigned to area V6A.

Behavioral paradigm. Monkeys performed an instructed-delay, fixate-to-hand lift task, as illustrated in Figure 1a-b and described previously (Breveglieri et al. 2012; 2014). Two types of trials were run in separate blocks: in one block the hand pressed a home button (HB) located next to its waist (Fig. 1a), whereas in the other the hand pressed another HB that was 14 cm farther along the mid-sagittal plane (Fig. 1b). For each neuron, the block sequence was randomized and only one HB was available for pressing. As a complete randomization of the trials of the two starting hand positions was not possible, a number of analyses were performed to account for potential confounds of signal instability (see below). Fixation targets were nine Light Emitting Diodes (LEDs) positioned at eye level, at three different distances and directions (Fig. 1a-b). Three LEDs targets were placed at three isovergence angles: the nearest targets were located at 10 cm from the eyes (17.1°) and the LEDs located at intermediate and far positions were at a depth (distance) of 15 cm (11.4°) and 25 cm (6.9°), respectively. At each isovergence angle LEDs were positioned in three directions: one central, along the sagittal midline and two lateral, at iso-version angles of -15° and +15°. It should be mentioned that, since the target was always on the fovea and the head of the animals was fixed, our experiment cannot distinguish body from head- and eye-centered frames of reference.

The time sequence of the task is shown in Figure 1c. A trial began when the monkey pressed a home button (HB press). After 1000 ms, one of the nine LEDs lit up green (LEDon) and the monkey had to fixate it, while maintaining the button pressed. Then, the monkey had to withhold any eye or hand movement for a variable delay period (1000 – 2000 ms) until the LED changed color (green to red). The color change was the go-signal (GO) for the animal to release the button in order to receive reward. A plexiglass wall was mounted on the chair in order to prevent reaching movements. **The arm used was contralateral to the recording hemisphere and in both monkeys neurons were recorded from both left and right hemispheres.**

The presentation of stimuli and the animal's performance were monitored using custom software written in Labview (National Instruments), as described previously (Kutz et al. 2003). Eye position signals were sampled with two cameras (one for each eye) of an infrared oculometer system (ISCAN) at 100 Hz and were controlled by an electronic window (4 x 4 degrees) centred on the fixation target. If the monkey fixated outside this window, the trial was aborted. The task was performed in darkness, in blocks of ninety randomized trials, ten for each LED target. The background light was switched on briefly between blocks to avoid dark adaptation.

Data Analysis. To check the stability of the recorded units between the two blocks, we computed the coefficient of variation (CV) in mean firing rate of trials for every block. CV **is defined as the ratio of the standard deviation to the mean of the interspike interval distribution**. The CV had to be <1.0 in each block to accept stability and validate the neural recording. **A CV less than 1.0 means that the spike train is more regular than a Poisson process with the same firing rate**. If one of the task blocks from a cell failed this validation, then the cell was rejected. The time interval used to calculate CV was the whole trial. The same

with T and H being part of the same function f and cannot be multiplicatively separated.

SVD is a method of linear algebra used to reconstruct a general, two-dimensional matrix M containing multivariate data. SVD reduces the matrix M into a weighted sum of products of two independent vectors, termed 'singular vectors'. The relative contribution of the products to the original matrix is quantified by their weights (s_1, s_2, etc), named 'singular values'. The method reduces M into another matrix, called N, using the formula:

$$N = USV^T$$

where S is a diagonal matrix containing singular values, and U and V are orthogonal matrices containing singular vectors.

From the Target-Hand (TH) matrices for each cell and epoch (i.e. the two-dimensional response matrix described above) we calculated the diagonal matrix S that contained the singular values:

with T and H being part of the same function f and cannot be multiplicatively separated.

SVD is a method of linear algebra used to reconstruct a general, two-dimensional matrix M containing multivariate data. SVD reduces the matrix M into a weighted sum of products of two independent vectors, termed 'singular vectors'. The relative contribution of the products to the original matrix is quantified by their weights (s_1, s_2, etc), named 'singular values'. The method reduces M into another matrix, called N, using the formula:

$$N = USV^T$$

where S is a diagonal matrix containing singular values, and U and V are orthogonal matrices containing singular vectors.

From the Target-Hand (TH) matrices for each cell and epoch (i.e. the two-dimensional response matrix described above) we calculated the diagonal matrix S that contained the singular values:

$$f(T, H) = s1t1(T)h1(H) + s2t2(T)h2(H) + \cdots.$$

If the first singular value is quite large compared to second and rest singular values, then the TH matrix can be reconstructed only by the first term of the equation above:

$$f(T, H) = s1\,t1(T)h1(H)$$

In this case, there is a gain relationship between T and H that shows multiplication. If instead the first singular value is not large enough compared to the rest, the modulation of the neural response by one variable (e.g. target) is affected by the position of the other variable (e.g. hand), thus the responses are inseparable. Neural

responses were classified as separable if the first singular value was significantly larger ($p<0.05$) compared to the first singular value calculated when conditions were randomized by permuting (Randomization test, 5000 permutations) the rows and the columns of the response matrix (Pesaran et al. 2006). In more detail, during the Randomization test the elements of the response matrix (i.e. the 18 mean firing rates, one per each condition) were permuted 5000 times and each rearranged matrix was subjected to SVD. The first singular values from all the rearranged matrices (N=5000) formed a distribution that was used to test for statistical significance. If the first singular value of the original matrix was greater than 95% of the singular values in this distribution, then the neural responses were classified as separable. A mean value, computed from all 18 conditions, was subtracted from each of the 18 mean firing rates of the response matrix elements before performing the SVD.

In conjunction with this analysis, we also used gradient analysis to assess whether a cell was significantly tuned and, if so, which of the two variables exerted the most influence on the firing rate of the cell (Buneo 2011; Buneo and Andersen 2012). **In this analysis the 2x9 matrix of mean firing rates was converted (using the Matlab function 'gradient') into a gradient i.e. a two-dimensional vector field that was plotted as red arrows in the left plots of Figure 2b-e. The directions and lengths of the set of red arrows indicate how the activity changes between matrix elements i.e. when the target and/or the initial hand position shift. The length of each arrow is numerically calculated as the gradient i.e. a derivative of the firing rate. Put together, they indicate the relative influence of target and hand position on the activity. For example, in the cell of Figure 2b most of the red arrows point to the left, illustrating the stronger effect of changes in target position (T) with respect to changes in initial hand position (H). Then in the circular plots to the right of each matrix, we summarized this information into a single resultant angle vector (or field orientation**

vector) that was computed by summing (vector addition) all the gradient elements i.e. all the individual red arrows. In some cases, matrices could show a symmetrical pattern of red arrows (some arrows pointing to the left/up and others to the right/down) that would cancel out during vector summation. To account for symmetric red arrows the angles of the red arrows were doubled (e.g. $\pi/2$ was converted to π) before being summed).

The result of this summation i.e. the resultant angle, was illustrated on circular plots from 0° to +/-180°. In Figure 2b-e each circular plot is shown with the interpretation of the relative strength of target (T) and hand (H) position: T at 0°, H at +/-180°, T-H at -90°, and T+H at +90°. **More specifically, resultant vectors pointing at 0° reflect a left/right pattern of red arrows and indicate a strong effect of target location T, whereas a resultant vector pointing +/-180° an upward/downward pattern and indicate a strong effect of initial hand position H. Resultant vectors with angles of +/-90° reflect a mixed pattern of red arrows. T-H is the difference between target and initial hand position that can be interpreted as encoding of target position in hand-centered coordinates. T+H does not have a straightforward interpretation (Buneo and Andersen 2012) and in fact there were very few cells with resultant vectors pointing at this orientation (see Results, Figure 5).** Each matrix was classified as tuned if the resultant length was significantly greater than the resultant length calculated after randomization of the matrix elements (**Gradient randomization test**). Rayleigh's test was used to assess the uniformity of circular histograms for tuned resultant angles ($p < 0.05$, with Bonferroni correction for multiple comparisons).

Figures 2b-e show the matrices and response fields for idealized cells with separable (Fig. 2b, c) and inseparable (Fig.2d, e) responses for target and hand variables. In the separable matrices there is strong tuning of activity by target position, with hand position having a weak (Fig.2b, left), or moderate (Fig. 2c, left) gain modulation effect on the spatial tuning. As a result, the response fields of these matrices point toward target position T (Fig.2b, right) and

midway between T and T-H (Fig.2c, right), according to the strength of gain modulation by hand position. In the inseparable matrices, the effects of target and hand position on activity cannot be accounted by a multiplicative coding mechanism, being either similar (Fig.2d, left), or hand position having a stronger effect on activity (Fig.2e, left). Accordingly, the response fields point toward T-H (Fig.2d, right), or toward H (Fig.2e, right).

A sliding window analysis was also performed to investigate the temporal evolution of responses along the task progress in more detail. Here the resultant length and orientation of the gradient was computed in each cell in 300 ms windows that moved in 50 ms steps. Firing rates were aligned to the start of fixation from 500 ms before to 700 ms after it, and to the Go signal from 500 ms before, to 700 ms after it. In the population sliding analysis, the mean resultant **was computed at each time step for every subpopulation i.e cell category defined according to the presence of tuning in the analysis epochs described above (see Results)**. Arrow lengths for the population analysis **were averaged (vector summation) within each subpopulation and therefore they were not comparable across subpopulations.**

Distinct patterns of frame of reference-related activity

Figure 3 shows an example neuron recorded with the fixate-to-hand lift task. Gradient analysis found this cell tuned only in the EARLY epoch. The early fixation firing activity of this neuron was low for near targets, gradually increased for intermediate targets and was maximal for the farthest target locations. This tuning was present in ipsilateral, central and contralateral space. **It should be mentioned that ipsilateral/central/contralateral space was defined with respect to the recording hemisphere.** More importantly, this strong spatial tuning was very weakly affected by the two different hand positions (compare discharge along the same column in Fig. 3a). The mean EARLY activity for this cell across **the 18 different trial conditions is illustrated in the matrix of Figure 3b as TH matrix. The TH matrix for this cell was separable (SVD Randomization test, $p<0.05$) with a resultant angle vector pointing at 3 degrees (Fig.3b, right panel, red arrow), indicating that the neural response was mainly affected by target position (compare with Fig.2b-c).** In the PLAN epoch this cell showed a decrease in firing for almost all target locations (with the exception of far contralateral targets) and, like in the EARLY epoch, changing hand position affected weakly the neural activity. Figure 3c shows the TH matrix with mean PLAN activity and the related response field. **The TH matrix was found to be separable with a resultant angle vector of -44 degrees (Fig.3c, right panel, red arrow), however it was not significantly tuned (Gradient randomization test, $p>0.05$).**

Figure 4a shows another cell recorded with the fixate-to-hand lift task that was tuned in both epochs. In the EARLY epoch the cell showed higher activity for far target locations in all parts of space, but this tuning was strong only when the animal pressed the near button location. When the hand position changed, the activity was higher for the near and intermediate

target in central and contralateral space, respectively. During the PLAN epoch the cell showed high activity for far contralateral and near central target locations that was diminished when hand position changed. The mean activity of this cell during the EARLY and PLAN epochs, across different trial conditions, is shown in the matrix of Figure 4b and 4c, respectively. Despite the lower firing rates in the PLAN epoch there was a strong influence of hand position in both matrices that were found to be inseparable. **Regarding the resultant angle vectors in the two epochs, they were found to be very similar (-172^0 vs -161^0; Fig.4b-c, red arrows in circular plots)**, indicating that the responses were more influenced by hand position.

In the fixate-to-hand lift task, gradient analysis revealed that 56 cells (68%) were significantly tuned in at least one of the two epochs. **Cells with tuning only in EARLY or PLAN epoch were named EARLY and PLAN cells, respectively, whereas neurons that were found tuned in both EARLY and PLAN epochs were termed as BOTH cells.** Subsequent SVD analysis found that the majority of EARLY cells (11/17) were separable. In contrast, almost all PLAN cells were inseparable. Sixteen out of the 24 BOTH cells were inseparable in both epochs, whereas only 2 cells were separable in both epochs. Regarding the remaining cells, three were separable in EARLY and inseparable in PLAN, and two cells showed the opposite pattern. The numbers of the various cell groups are reported in Table 1, **also separately for each animal. Given the very low number of cells in Monkey B it was not possible to perform a statistical comparison of the results in the two monkeys. However, though few, the cells in Monkey B were all inseparable, therefore the main trend of inseparable cells was present in both animals.**

Figure 5a shows the distributions of the resultant angles for inseparable (top) and separable (bottom) tuned neurons. Most separable neurons had resultant angles that indicated a predominant effect of target location (Fig.5a, bottom panels, arrows pointing towards "T"). In comparison, inseparable neurons showed a complementary distribution

of resultant angles that ranged from those indicating an encoding of target relative to hand position (Fig.5a, top panels, arrows pointing towards "T-H", see also Methods) to the ones suggesting a predominant effect of hand position (Fig.5a, top panels, arrows pointing towards "H"). Regarding the subpopulations of EARLY, PLAN and BOTH cells, we observed a distinct pattern of the distributions. Separable and inseparable BOTH cells showed a very limited range of resultant angle orientations that indicated a strong effect of initial hand position (Fig.5A, right top and bottom panels, arrows pointing towards "H"). PLAN cells had a more uniform distribution of resultant angles with separable neurons pointing primarily towards "T" (weak and strong gain fields) and inseparable ones distributed from "T-H" to "H". EARLY cells were mostly distributed between "T" and "T-H", with a clear bias towards "T". Regarding the temporal progress of separable/inseparable responses in cells tuned in both epochs we found that responses were consistent in the vast majority of cases (19/24). In addition, they had very similar field orientation (Fig.5b). Taken together, the epoch analysis revealed two major trends in the population recorded with the fixate-to-hand lift task: a) cells with sustained (BOTH cells) or late tuning (PLAN cells) that showed a strong tendency to be inseparable and had a strong influence of hand position and b) cells with only early tuning (EARLY cells) that tended to show separable tuning and were more strongly affected by target location.

We applied the same gradient and SVD analyses to another population of V6A cells **(n=240, Monkey A/B: 146/94) recorded in the same monkeys** during the fixate-to-reach task under identical target and initial hand position configuration. In this task about 80% of neurons were significantly tuned in at least one of the EARLY, PLAN or REACH epochs (Table 1). Based on the presence or absence of tuning in REACH epoch, cells can be grouped into three main categories: a) Cells tuned only in REACH epoch, b) cells not tuned in REACH, but in either EARLY or PLAN, or in both of them, c) cells with tuning both in REACH and in either EARLY

or PLAN, or in both of them. In all these groups the vast majority of cells were found to be inseparable. This finding is similar to our results from the fixation task for cells tuned in PLAN only and in both EARLY and PLAN epochs, but not for the EARLY cells that were mostly separable. Thus, the encoding of the two variables in EARLY tuned cells differed between the two tasks and this difference was statistically significant (two-sample binomial test, $p<0.05$). The numbers of the separable and inseparable cells**, per animal,** are reported in Table 1.

Another aspect of the fixate-to-reach task analysis regarded the consistency of responses in the groups of cells with tuning in multiple epochs. In each of these groups, more than half of the cells showed the same tuning across epochs, with the inseparable responses being the most frequent (Table 1). These results show that, similar to the fixation task, during the fixate-to-reach task the responses of cells are mostly inseparable and show consistency across epochs.

Temporal evolution of the frames of reference in the two tasks

To investigate the temporal evolution of responses in finer detail, we conducted a sliding window analysis **(300-ms window, 50-ms step, see also Methods)** of gradient response fields during the task, starting from the period that the animal acquired the initial hand position, i.e. before the target appearance till the end of the trial. Figure 6 illustrates the results of this analysis for the three populations of cells: EARLY, PLAN and BOTH recorded during the fixate-to-hand lift task. Each data point plots the angle of population's response field orientation, thus indicating which of the two variables has a stronger effect on activity at each time step. The distance of each point from the centre of the circle indicates the strength of tuning at that point in time. Data were aligned to the start of fixation (left panels) and Go cue appearance (right panels). Figure 6a shows the temporal evolution of the population response in EARLY cells. As shown in the left panel of the figure, there was a strong influence of hand position in the period before the target presentation (Fig.6a, left, blue data points).

Subsequently, around the time of the saccade and just after the target was fixated the population orientation angle shifted to encode mainly the target position (Fig.6a, left, green data points). In the late part of EARLY epoch and in the 200 ms after it (Fig.6a, left, green data points), the strength of target coding decayed and the orientation of response field moved towards intermediate –between target and hand- angles. In the right panel of Figure 6a, the population response of the EARLY cells is shown during the interval starting from the PLAN epoch, until the end of the trial. During the PLAN epoch (Fig.6a, right, blue data points), the magnitude of the population resultant vector was small in line with the absence of tuning in this group during PLAN, as expected for this cell class. Interestingly, after the Go cue and around the button release event (Fig.6a, right, green and yellow data points), the strength of tuning gradually increased and the orientation of the population response indicated a main effect of hand position. In sum, the population response of EARLY cells showed a substantial flexibility across the time course of the trial with strong influence of hand position in the beginning and at the end of the trial and significant coding of target information around the saccade and in early fixation period.

The dynamics of population response in the cells tuned in PLAN was different (Fig.6b). Before target appearance there was a strong influence of hand position in this group (Fig.6b, left, dark blue data points), similarly to the EARLY population. Around the saccade the response decayed and slightly shifted, indicating a small effect of target position (Fig.6b, left, light blue and dark green data points) and it further decreased in the subsequent part of the EARLY epoch (Fig.6b, left, yellow data points). In the PLAN period, the population response was initially moderate with a very strong orientation bias towards hand position (Fig.6b, right, blue data points) and it further decreased in the late part of PLAN (Fig.6b, right, blue data points). After the Go cue there was a gradual increase in the strength of the response and a shift in orientation, thus suggesting a small influence of target position (Fig.6b, right, green data

points). Around the time of the hand releasing the button, the population response further increased its strength and shifted back to representing almost exclusively hand position (Fig.6b, right, dark yellow data points) and it decayed towards the end of the trial (Fig.6b, right, light yellow data points). The weaker population response of PLAN cells during PLAN epoch compared to the subsequent reaction time and hand action periods could be the result of a population of cells with a bimodal distribution with individual cell vectors cancelling out during averaging. Alternatively, it could reflect a real increase in strength of tuning closer to the manual response.

In contrast to the EARLY and PLAN cells, there was no shift in the population response orientation in BOTH cells with the vector pointing always towards "H" (Fig.6c). Before target appearance, the magnitude of the response was close to maximum. Its peak was observed just after the saccade and it slightly decayed at the end of the EARLY period (Fig.6c, left). Similarly, during the PLAN epoch the response was close to its peak level, reached it just before and during the hand lifting off the button and then decayed toward the end of the trial.

As similar analyses were performed for the V6A neurons recorded fixate-to-reach task, Figure 7 shows the tuning orientation and strength of the population response across time in the main subpopulations recruited in this task. In all cases, a sustained prevalent effect of hand position was observed, with target location exerting a weaker and transient influence around the occurrence of main task events i.e. fixation onset, Go signal and movement execution (Fig.7, top panels). In contrast, this small effect was absent in the cells tuned in all three epochs (Fig.7, bottom panels), with the population vectors pointing always towards "H".

In sum, these findings show that neural populations in V6A involved in a visuospatial (fixate-to-hand lift) and in a reaching (fixate-to-reach) task show similar frames of reference. In both populations, the responses of single neurons were in most part inseparable, thus

indicating a mixed encoding of target location and hand position signals, with the latter being stronger in most task phases. Moreover, in neurons tuned in multiple epochs the reference frames were stable. The only difference in reference frames we observed between the two tasks regarded the recruitment of cells in the early stages of the task (epoch EARLY), where the responses were mostly separable in the fixate-to-hand lift task and inseparable in the fixate-to-reach task.

Discussion

We characterized the reference frames in area V6A at several points during the execution of a fixate-to-hand lift task, both at the level of single neurons and that of physiologically defined subpopulations. We also applied the same analyses to a dataset of V6A cells recorded during a fixation-to-reach task, and compared the results between the two tasks. Using the first task, we observed subpopulations of neurons that were differentially modulated over distinct time intervals across the task progress. Cells that were tuned only for 500 ms after fixation onset (EARLY) showed mostly separable responses, with their population response influenced primarily by target position. This suggests a strong effect of pure visuospatial signals. Differently, cells which showed tuning in later stages (PLAN) and those with sustained tuning across the task revealed predominantly inseparable responses at the single cell level, and a stronger contribution of hand position signals on the pooled subpopulation response. These two later properties were also characteristic of another population of V6A neurons recorded during the fixate-to-reach task.

Time course of population activity

In the fixate-to-hand lift task, the vector of pooled response in EARLY cells around fixation onset pointed towards target position (Fig.6a), thus indicating a strong bias towards body-centered coordinates, **which, in our experimental design (e.g. head-fixed and reach targets were foveated), were equivalent to head- and eye-centered coordinates**. However, to classify the subpopulations of PLAN and BOTH cells as hand-centered, the average resultant vectors should point towards the target minus hand (T-H) orientation, a result that was not found to be the case (Fig.6b-c). As a result, rather than hand-centered coding, the pooled population responses in PLAN and BOTH subpopulations is indicative of mixed, intermediate coding with the hand position signals being dominant. The strong presence of hand signals was

evident in all three subpopulations also before the target appearance (see dark blue points in Fig.6), suggesting the coding of hand posture information. The high incidence of intermediate reference frames and the prevalence of hand position signals were also observed in the population of V6A neurons recorded during a fixate-to-reach task (Fig.7). In sum, the present findings suggest that medial PPC uses consistent reference frames that are not significantly affected by the presence or absence of spatially-directed motor responses.

Comparison with previous studies

In our study eye position always covaried with target position, so body/head-centered coordinates were equivalent to eye-centered. Similarly, we cannot determine whether the mixed target and hand position coding was also influenced by eye position signals. Previous studies of reference frames in V6A during 3D reaches where eye position was uncoupled from reach target location reported intermediate eye- and body-centered coding (Bosco et al., 2015; Bosco et al., 2016). In addition, there are earlier studies of coordinate frames in PPC in which activity was recorded during center-out reaches in the medial intraparietal cortex, both within the sulcus (area MIP) and in the exposed surface (area PE; Pesaran et al. 2006; Bremner et al. 2012). Using an array of target and initial eye/hand positions, several populations of cells affected by eye and/or hand signals were reported (Pesaran et al. 2006; Bremner et al. 2012). Although a bias for eye-centered representations in MIP and hand-centered representations in PE was observed, in MIP the coding of target location was affected by hand position signals in a large number cells. Unlike our results, in the majority of MIP cells the responses during the planning period were separable, and the pooled population response showed a bias towards target position (see Fig.7h in Pesaran et al. 2006), suggesting that, compared to V6A, hand position signals have a weaker influence in MIP. A majority of separable responses was found also in another MIP study in which the integration of target and hand position signals was investigated across different workspaces (Buneo and Andersen,

2012). Differently, in both our tasks most V6A responses were inseparable, and could not be fully accounted for either by a hand-centered reference frame, or by a hand position gain field, thus suggesting a mixed reference frame.

Differences between V6A and MIP could reflect real functional differences between these areas, which are distinct in terms of connections and myeloarchitecture (Bakola et al. 2017). However, methodological differences also need to be kept in mind. First, in MIP studies center-out reaches were performed with various (left/right and/or up/down) movement trajectories that were always constrained in a two-dimensional plane, whereas in the present study targets were distributed in various directions and distances, and upward reaches of various directions and amplitudes were also performed. Second, in previous MIP studies hand and target position were manipulated in the same frontoparallel plane, whereas here they were varied at different depth planes. There is evidence from human psychophysics studies suggesting that the proprioceptive input from the hand is stronger in the depth dimension compared to direction (Vindras et al., 1998; van Beers et al., 2004; Apker et al., 2010). Accordingly, the changing of hand and target position in depth in our experiment is likely to involve more proprioceptive (inseparable) coding of target location with respect to the hand, compared to the visual (separable) coding of direction difference between target and hand location in MIP. To determine whether MIP is similar to V6A and shows an inseparable coding in 3D space, the same tasks will need to be applied while recording from cells in both these areas.

To our knowledge, the only study in which the effects of manipulating the starting hand position in depth on reach-related activity were examined was conducted in area PE (Ferraina et al. 2009). In that work, a multiple linear regression analysis found that activity in most cells was correlated with the movement distance in both body- and hand-centered coordinates, although fitting with hand movement vector gave slightly better fits. This finding suggests the

presence of intermediate coding between body- and hand- centered frames, in agreement with our present results in both tasks. In previous studies of 3D reaches with varying initial hand position we found the same type of intermediate coding -both in V6A and neighboring area PEc- using a diverse set of analysis methods such as Euclidean Distance (Batista et al. 2007) and Vector Correlation (Buneo 2011; Buneo and Andersen 2012; Hadjidimitrakis et al. 2014a; Piserchia et al. 2017). Despite the fact that depth and direction signals are processed in overlapping neural populations in some PPC areas like V6A and PEc (Hadjidimitrakis et al. 2014a; 2015; Hadjidimitrakis et al. 2019), it seems that the neural mechanisms of spatial coding in 2D and 3D space are different. At this regard, several theoretical and modeling studies suggest that the intermediate representations could be beneficial to the computations that are necessary for the coordinates transformation in 3D space (Pouget and Snyder, 2000; Blohm et al., 2009; 2012).

Functional considerations

Mixed reference frames have been considered important for providing flexibility in the spatial computations performed under different behavioral contexts and task conditions (Chang and Snyder 2010; McGuire and Sabes 2011). Evidence from both human and monkey studies suggest changes in the neural encoding of eye and arm/hand movements depending on sensory input and task demands (Bernier and Grafton 2010; Pesaran et al. 2010; Lee and Groh 2012; Leone et al. 2015), whereas other studies reported that reference frames were independent of the sensory modality of the target (Mullette-Gillman et al., 2005; 2009; McGuire and Sabes, 2011; Buneo and Andersen, 20

Pesaran and colleagues (2010) compared the spatial representations of the planning activity between center out reaches and saccades in PMd neurons with the same manipulation of eye and hand starting positions and perfomed SVD and gradient analysis. In the saccade

2008; Chang and Snyder 2010; McGuire and Sabes 2011; Bremner and Andersen 2014; Hadjidimitrakis et al. 2017). Both in single neurons and averaged population responses we found limited evidence for changes in reference frames during the task evolution. **However, the gradual change of resultant angles in EARLY (from T till T-H) and PLAN (from T-H till H) cells during the fixate-to hand-lift task (see Fig.5a, compare arrows between middle top and bottom left panels) suggests that these subpopulations of cells recruited at different task intervals could underlie the different stages of the reference frame transformation during reaching movements i.e. the shift of target location encoding from eye- or body/head-centered to hand-centered coordinates.**

Funding

This work was supported by National Health and Medical Research Council (Australia, 1082144), European Union (H2020-MSCA-734227–PLATYPUS), Ministero dell'Università e della Ricerca (MIUR) National Research Project (Italy, PRIN2017KZNZLN) and Fondazione Cassa di Risparmio in Bologna (Italy).

Acknowledgments

This paper is part of a special issue celebrating Jack Pettigrew's seminal contributions to science. Jack's studies were central to revealing the physiological bases of stereo vision (e.g. Pettigrew et al. 1968), which can be rightfully be considered a cornerstone of current understanding of perception and action in 3 dimensions. One of the senior authors of this paper (MGPR) has had the privilege of working with Jack, and acknowledges his key contribution to defining his scientific career.

The authors thank Drs. F. Bertozzi and G. Dal Bo' for help in the recordings. We thank Drs L. Passarelli and M. Gamberini for help with surgery and histological reconstruction of penetrations, and M. Verdosci for mechanical assistance. Conflicts of interest: None declared.

Data Availability Statement

Research data are available upon reasonable request.

References

Apker GA, Darling TK, Buneo CA. 2010. Interacting Noise Sources Shape Patterns of Arm Movement Variability in Three-Dimensional Space. J Neurophysiol 104: 2654-2666.Battaglia-Mayer A, Ferraina S, Genovesio A, Marconi B, Squatrito S, Molinari M, Lacquaniti F, Caminiti R. 2001. Eye-hand coordination during reaching. II. An analysis of the relationships between visuomanual signals in parietal cortex and parieto-frontal association projections. Cereb Cortex. 11: 528-544

Batista AP, Buneo CA, Snyder LH, Andersen RA (1999) Reach plans in eye-centered coordinates. Science 285:257-260.

Batista AP, Santhanam G, Yu BM, Ryu SI, Afshar A, Shenoy KV (2007) Reference frames for reach planning in macaque dorsal premotor cortex. Journal of neurophysiology 98:966-983.

Bernier PM, Grafton ST (2010) Human posterior parietal cortex flexibly determines reference frames for reaching based on sensory context. Neuron 68:776-788.

Blohm G, Keith GP, Crawford JD. 2009. Decoding the Cortical Transformations for VisuallyGuided Reaching in 3D Space. Cereb Cortex 19: 1372-1393.

Blohm G (2012) Simulating the Cortical 3D Visuomotor Transformation of Reach Depth. PLoS One 7:e41241.

Bosco A, Breveglieri R, Reser D, Galletti C, Fattori P (2015) Multiple representation of reaching space in the medial posterior parietal area V6A. Cerebral cortex 25:1654-1667.

Bosco A, Breveglieri R, Hadjidimitrakis K, Galletti C, Fattori P (2016) Reference frames for reaching when decoupling eye and target position in depth and direction. Scientific reports 6:21646.

Boussaoud, D., & Wise, S. P. (1993). Primate frontal cortex: effects of stimulus and movement. Exp Brain Res, 95(1), 28-40.

Bremner L, Andersen R (2012) Coding of the Reach Vector in Parietal Area 5d. Neuron 75:342-351.

Bremner LR, Andersen RA (2014) Temporal analysis of reference frames in parietal cortex area 5d during reach planning. The Journal of neuroscience : the official journal of the Society for Neuroscience 34:5273-5284.

Breveglieri R., Hadjidimitrakis K., Bosco A., Sabatini S. P., Galletti C., Fattori P. (2012). Eye Position Encoding in Three-Dimensional Space: Integration of Version and Vergence Signals in the Medial Posterior Parietal Cortex. J Neurosci 32, 159-169

Breveglieri R., Galletti C., Dal Bo G., Hadjidimitrakis K., Fattori P. (2014). Multiple aspects of neural activity during reaching preparation in the medial posterior parietal area V6A. J Cogn Neurosci 26, 878-895
Buneo CA, Batista A, Jarvis M, Andersen R (2008) Time-invariant reference frames for parietal reach activity. Experimental brain research 188:77-89.
Buneo CA. 2011. Analyzing neural responses with vector fields. J Neurosci Methods. 197:109–117.
Buneo CA, Andersen RA (2012) Integration of target and hand position signals in the posterior parietal cortex: effects of workspace and hand vision. Journal of neurophysiology 108:187-199.
Buneo CA, Jarvis MR, Batista AP, Andersen RA (2002) Direct visuomotor transformations for reaching. Nature 416:632-636.
Chang SWC, Snyder LH (2010) Idiosyncratic and systematic aspects of spatial representations in the macaque parietal cortex. Proceedings of the National Academy of Sciences 107:7951-7956.
Chen X, DeAngelis GC, Angelaki DE (2018). Flexible egocentric and allocentric representations of heading signals in parietal cortex. Proc Natl Acad Sci U S A. 115:E3305-E3312.
di Pellegrino, G., & Wise, S. P. (1993). Visuospatial versus visuomotor activity in the premotor and prefrontal cortex of a primate. J Neurosci, 13(3), 1227-1243.
Ferraina S, Brunamonti E, Giusti MA, Costa S, Genovesio A, Caminiti R. 2009. Reaching in Depth: Hand Position Dominates over Binocular Eye Position in the Rostral Superior Parietal Lobule. J Neurosci 29: 11461-11470.
Filippini, M., Breveglieri, R., Hadjidimitrakis, K., Bosco, A., and Fattori, P. (2018). Prediction of Reach Goals in Depth and Direction from the Parietal Cortex. Cell Rep. 23, 725–732
Flanders M, Helms Tillery SI, Soechting JF (1992) Early stages in a sensorimotor transformation. Behav Brain Sci 15:309-362.
Galletti C, Battaglini PP, Fattori P (1995) Eye position influence on the parieto-occipital area PO (V6) of the macaque monkey. Eur J Neurosci 7:2486-2501.
Galletti C, Fattori P, Kutz DF, Gamberini M (1999) Brain location and visual topography of cortical area V6A in the macaque monkey. Eur J Neurosci 11:575-582.
Galletti C, Fattori P, Battaglini PP, Shipp S, Zeki S (1996) Functional demarcation of a border between areas V6 and V6A in the superior parietal gyrus of the macaque monkey. Eur J Neurosci 8:30-52.
Gamberini M, Dal Bò G, Breveglieri R, Briganti S, Passarelli L, Fattori P Galletti C (2018) Sensory Properties of the Caudal Aspect of the Macaque Superior Parietal Lobule Brain Structure and Function, 223:1863-1879
Hadjidimitrakis K, Breveglieri R, Placenti G, Bosco A, Sabatini SP, Fattori P. 2011. Fix Your Eyes in the Space You Could Reach: Neurons in the Macaque Medial Parietal Cortex Prefer Gaze Positions in Peripersonal Space. PLoS ONE. 6: e23335.
Hadjidimitrakis K, Breveglieri R, Bosco A, Fattori P (2012) Three-dimensional eye position signals shape both peripersonal space and arm movement activity in the medial posterior parietal cortex. Frontiers in integrative neuroscience 6:37.
Hadjidimitrakis K, Bertozzi F, Breveglieri R, Fattori P, Galletti C (2014a) Body-centered, mixed, but not hand-centered coding of visual targets in the medial posterior parietal cortex during reaches in 3D space. Cerebral cortex 24:3209-3220.
Hadjidimitrakis K, Bertozzi F, Breveglieri R, Bosco A, Galletti C, Fattori P (2014b) Common neural substrate for processing depth and direction signals for reaching in the monkey medial posterior parietal cortex. Cerebral cortex 24:1645-1657.

Hadjidimitrakis K, Dal Bo' G, Breveglieri R, Galletti C, Fattori P. Overlapping representations for reach depth and direction in caudal superior parietal lobule of macaques. J Neurophysiol. 2015 Oct;114(4):2340–52.
Hadjidimitrakis K, Bertozzi F, Breveglieri R, Galletti C, Fattori P (2017). Temporal stability of reference frames in monkey area V6A during a reaching task in 3D space. Brain Structure and Function, 222:1959-1970.
Hadjidimitrakis K, Bakola S, Wong YT, Hagan MA (2019). Mixed Spatial and Movement Representations in the Primate Posterior Parietal Cortex. Frontiers in Neural Circuits 13:15
Hayhoe MM, Shrivastava A, Mruczek R, Pelz JB (2003) Visual memory and motor planning in a natural task. Journal of vision 3:49-63.
Heider B, Karnik A, Ramalingam N, Siegel RM. 2010. Neural Representation During Visually Guided Reaching in Macaque Posterior Parietal Cortex. J Neurophysiol. 104: 3494-3509.
Johansson RS, Westling G, Backstrom A, Flanagan JR (2001) Eye-hand coordination in object manipulation. The Journal of neuroscience : the official journal of the Society for Neuroscience 21:6917-6932.
Kutz DF, Fattori P, Gamberini M, Breveglieri R, Galletti C (2003) Early- and late-responding cells to saccadic eye movements in the cortical area V6A of macaque monkey. Experimental brain research 149:83-95.
Kutz DF, Marzocchi N, Fattori P, Cavalcanti S, Galletti C (2005) Real-Time Supervisor System Based on Trinary Logic to Control Experiments With Behaving Animals and Humans. Journal of neurophysiology 93:3674-3686.
Lee J, Groh JM (2012) Auditory signals evolve from hybrid- to eye-centered coordinates in the primate superior colliculus. J Neurophysiol. 108:227-42.
Leone FT, Monaco S, Henriques DY, Toni I, Medendorp WP (2015) Flexible Reference Frames for Grasp Planning in Human Parietofrontal Cortex(1,2,3). eNeuro 2.
Luppino G, Ben Hamed S, Gamberini M, Matelli M, Galletti C (2005) Occipital (V6) and parietal (V6A) areas in the anterior wall of the parieto-occipital sulcus of the macaque: a cytoarchitectonic study. European Journal of Neuroscience 21:3056-3076.
Marzocchi N, Breveglieri R, Galletti C, Fattori P (2008) Reaching activity in parietal area V6A of macaque: eye influence on arm activity or retinocentric coding of reaching movements? Eur J Neurosci 27:775-789.
McGuire LM, Sabes PN (2011) Heterogeneous representations in the superior parietal lobule are common across reaches to visual and proprioceptive targets. The Journal of neuroscience : the official journal of the Society for Neuroscience 31:6661-6673.
Mullette-Gillman ODA, Cohen YE, Groh JM. 2005. Eye-Centered, Head-Centered, and Complex Coding of Visual and Auditory Targets in the Intraparietal Sulcus. J Neurophysiol 94: 2331-2352.
Mullette-Gillman ODA, Cohen YE, Groh JM (2009) Motor-Related Signals in the Intraparietal Cortex Encode Locations in a Hybrid, rather than Eye-Centered Reference Frame. Cereb Cortex 19:1761-1775
Pettigrew JD, Nikara T, Bishop PO (1968) Binocular interaction on single units in cat striate cortex: Simultaneous stimulation by single moving slit with receptive fields in correspondence Exp Brain Res 6: 391-410
Pesaran B, Nelson MJ, Andersen RA (2006) Dorsal Premotor Neurons Encode the Relative Position of the Hand, Eye, and Goal during Reach Planning. Neuron 51:125-134.
Pesaran B, Nelson MJ, Andersen RA (2010) A relative position code for saccades in dorsal premotor cortex. J Neurosci 30:6527–6537

Piserchia V, Breveglieri R, Hadjidimitrakis K, Bertozzi F, Galletti C, Fattori P (2017) Mixed Body/Hand Reference Frame for Reaching in 3D Space in Macaque Parietal Area PEc. Cereb Cortex. 27:1976-1990.
Pouget A, Snyder LH (2000) Computational approaches to sensorimotor transformations. Nat Neurosci 3 Suppl:1192-1198.
Pouget A, Deneve S, Duhamel JR (2002) A computational perspective on the neural basis of multisensory spatial representations. Nature reviews Neuroscience 3:741-747.
Reyes-Puerta V, Philipp R, Lindner W, Hoffmann KP. (2010) Role of the rostral superior colliculus in gaze anchoring during reach movements. J Neurophysiol. 103:3153-66.
Sajad A, Sadeh M, Yan X, Wang H, Crawford JD (2016) Transition from Target to Gaze Coding in Primate Frontal Eye Field during Memory Delay and Memory-Motor Transformation. eNeuro.3(2) e0040-16.2016 1–20.
Thura D, Boussaoud D, MeunierM (2008a) Hand position affects saccadic reaction times in monkeys and humans. J Neurophysiol 99:2194 –2202.
Thura D, Hadj-Bouziane F, Meunier M, Boussaoud D (2008b) Hand position modulates saccadic activity in the frontal eye field. Behav Brain Res 186:148 –153
van Beers RJ, Haggard P, Wolpert DM. 2004. The role of execution noise in movement variability. J Neurophysiol 91: 1050-1063.
Vindras P, Desmurget M, Prablanc C, Viviani P. 1998. Pointing errors reflect biases in the perception of the initial hand position. J Neurophysiol 79: 3290-3294.
Zipser D, Andersen RA (1988) A back-propagation programmed network that simulates response properties of a subset of posterior parietal neurons. Nature 331:679-684.

Table 1. Incidence of separable and inseparable tuning in each task and epoch.

Fixate-to-hand lift (n=56/76)

EARLY (n=17)	PLAN (n=15)	BOTH (n=24)
6(5-1)/**11(11-0**)	13(12-1)/**2(2-0)**	16(14-2)/**3(3-0)**

Fixate–to-reach (n=193/240)

EARLY (n=22)	PLAN (n=13)	BOTH (n=10)	
16(10-6)/**6(5-1)**	10(8-2)/**3(1-2)**	8(5-3)/**2(2-0)**	
REACH (n=49)	ALL (n=51)	EARLY- REACH (n=23)	PLAN-REACH (n=25)
37(19-18)/**12(9-3)**	26(16/10)/**7(5-2)**	11(3/8)/**3(1-2)**	12(8-4)/**3(2-1)**

The number of tuned inseparable and tuned separable (in bold) neurons for each epoch and task is reported. **Number pairs in parentheses denote the number of cells in the two animals (A-B)**. Asterisks indicate a statistical difference between the 2 animals. Comparing the relative proportions of separable and inseparable cells in the various subpopulations across tasks showed a significant difference only in the cells tuned in epoch EARLY (two-sample binomial test, $p<0.05$).

Figure Legends

Fig.1. Experimental arrangement and task sequence.

a, b: Side (top) and top (bottom) view of the reaching in depth set up task. Eye movements and button releases were performed in darkness towards one of the 9 LEDs located at eye level at different depths and directions from one hand position located next to the body and another being 14 cm farther.

c: Time sequence of task events with LED and hand status, the eye's vergence and version traces during a single trial. From left to right vertical continuous lines indicate: trial start (HB press), target appearance (LED), fixation onset (Fix), go signal (GO) and the start of the hand lift period (HB release) that marks the trial's end.

Fig.2. Gradient and separability analysis of modelled neural responses.

a. Spatial arrangement of hand and target combinations used in the response matrices in panels **B-**

b-e. Idealized neural responses.

b: Weak modulation (gain field) of target position (T) coding by hand position (H). **c**: Moderate gain field of H on T. **d**: Vector relationship between H and T, also referred to as hand-centered coding. **e**: Intermediate coding between H and T, characterized by a strong effect of H on target position (T) coding.

Left panels show idealized matrix responses for the H and T pair of variables. White represents a high firing rate and black represents a low firing rate. Small red arrows show the gradient of each matrix response field. Right panels show the overall response field

orientation calculated from the red gradient arrows. The response field orientation indicates the relative influence of each variable on the firing rate of the cell.

Fig.3. Example neuron showing tuning only in EARLY epoch.

a: Rasters and spike density functions of the neuron for the 9 target positions arranged as illustrated in the schematic above while the hand pressed and then released a button at a far (upper panels) and near (lower panels) location. Vertical lines indicate the alignment of activity at the start of fixation (Fix; left) and at the Go signal (Go; right).

b-c: Response matrices (left) and gradient resultant angle orientation (right) fields of the neuron shown in A during EARLY **(b)** and PLAN **(c)** epoch. In the response matrices, mean firing activity for each condition is plotted as a difference from the mean of all conditions.

Fig.4. Example neuron showing tuning in both EARLY and PLAN epoch. All figure conventions were as in Fig.3.

Fig.5. Resultant angle vectors for all the tuned cells **(n=56)** in the EARLY and/or PLAN epochs.

a. Numbers indic te the number of neurons in each plot, with the number of best tuned neurons in parentheses. Red vectors represent the mean of the black vectors in each plot. In BOTH cells the orientation during PLAN epoch is shown. **Please note that in some cases several neurons had very similar resultant angles (e.g. BOTH inseparable cells thick black arrows below red arrow).**

b. Angle difference between **resultant angle vectors** in the cells tuned in both EARLY and PLAN.

Fig.6. Temporal evolution of reference frames for the population of EARLY-only (**a**), PLAN-only (**b**) and both (**c**) cells active during the fixation-to-hand lift task. In each circular plot, the colored dots represent the average resultant for the each population of cells at 50-ms time steps (300 ms window). The direction of each dot in the circular plot indicates the mean orientation and its distance from the center the strength of tuning. Tuning strength is normalized within each subpopulation and the data were aligned to fixation onset (left plots) and Go cue (right plots).

Fig.7. Temporal evolution of reference frames for the main subpopulations of cells active during the fixation-to-reach task. At the top row data were aligned at fixation onset (left) or at the Go cue (middle and right). Same conventions as in Figure 6.

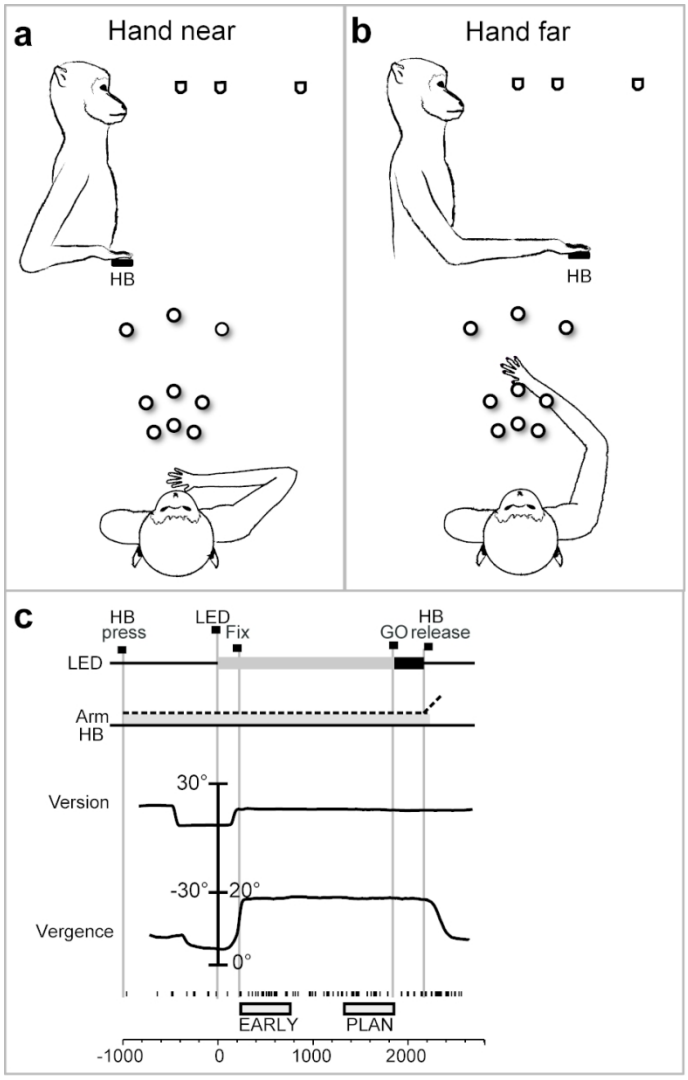

Figure 1

Fig.1. Experimental arrangement and task sequence.
a, b: Side (top) and top (bottom) view of the reaching in depth set up task. Eye movements and button releases were performed in darkness towards one of the 9 LEDs located at eye level at different depths and directions from one hand position located next to the body and another being 14 cm farther.
c: Time sequence of task events with LED and hand status, the eye's vergence and version traces during a single trial. From left to right vertical continuous lines indicate: trial start (HB press), target appearance (LED), fixation onset (Fix), go signal (GO) and the start of the hand lift period (HB release) that marks the trial's end.

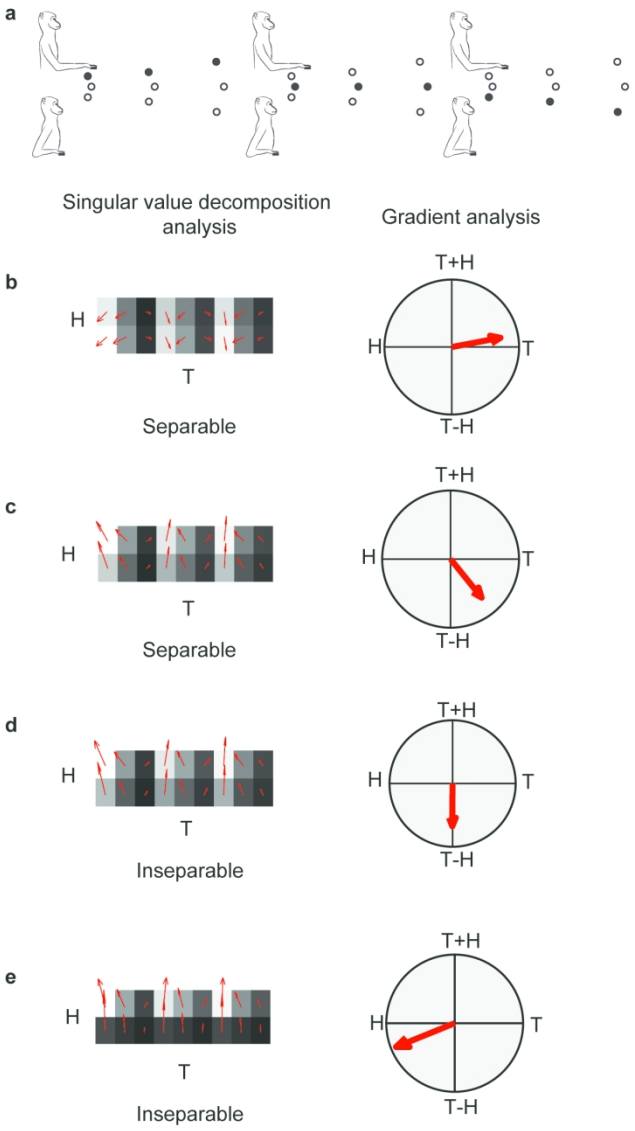

Figure 2

Fig.2. Gradient and separability analysis of modelled neural responses.
a. Spatial arrangement of hand and target combinations used in the response matrices in panels B-E.
b-e. Idealized neural responses.
b: Weak modulation (gain field) of target position (T) coding by hand position (H). c: Moderate gain field of H on T. d: Vector relationship between H and T, also referred to as hand-centered coding. e: Intermediate coding between H and T, characterized by a strong effect of H on target position (T) coding.
Left panels show idealized matrix responses for the H and T pair of variables. White represents a high firing rate and black represents a low firing rate. Small red arrows show the gradient of each matrix response field. Right panels show the overall response field orientation calculated from the red gradient arrows. The response field orientation indicates the relative influence of each variable on the firing rate of the cell.

108x205mm (300 x 300 DPI)

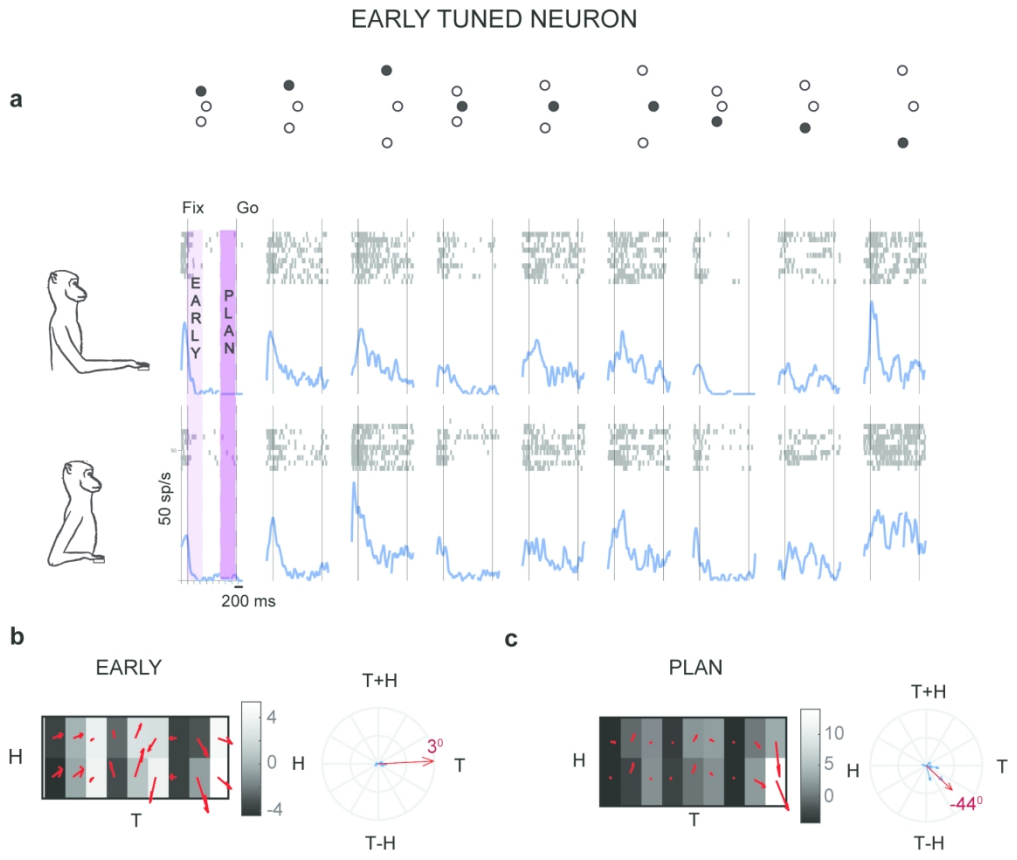

Figure 3

Fig.3. Example neuron showing tuning only in EARLY epoch.
a: Rasters and spike density functions of the neuron for the 9 target positions arranged as illustrated in the schematic above while the hand pressed and then released a button at a far (upper panels) and near (lower panels) location. Vertical lines indicate the alignment of activity at the start of fixation (Fix; left) and at the Go signal (Go; right).
b-c: Response matrices (left) and gradient resultant angle orientation (right) fields of the neuron shown in A during EARLY (b) and PLAN (c) epoch. In the response matrices, mean firing activity for each condition is plotted as a difference from the mean of all conditions.

169x163mm (300 x 300 DPI)

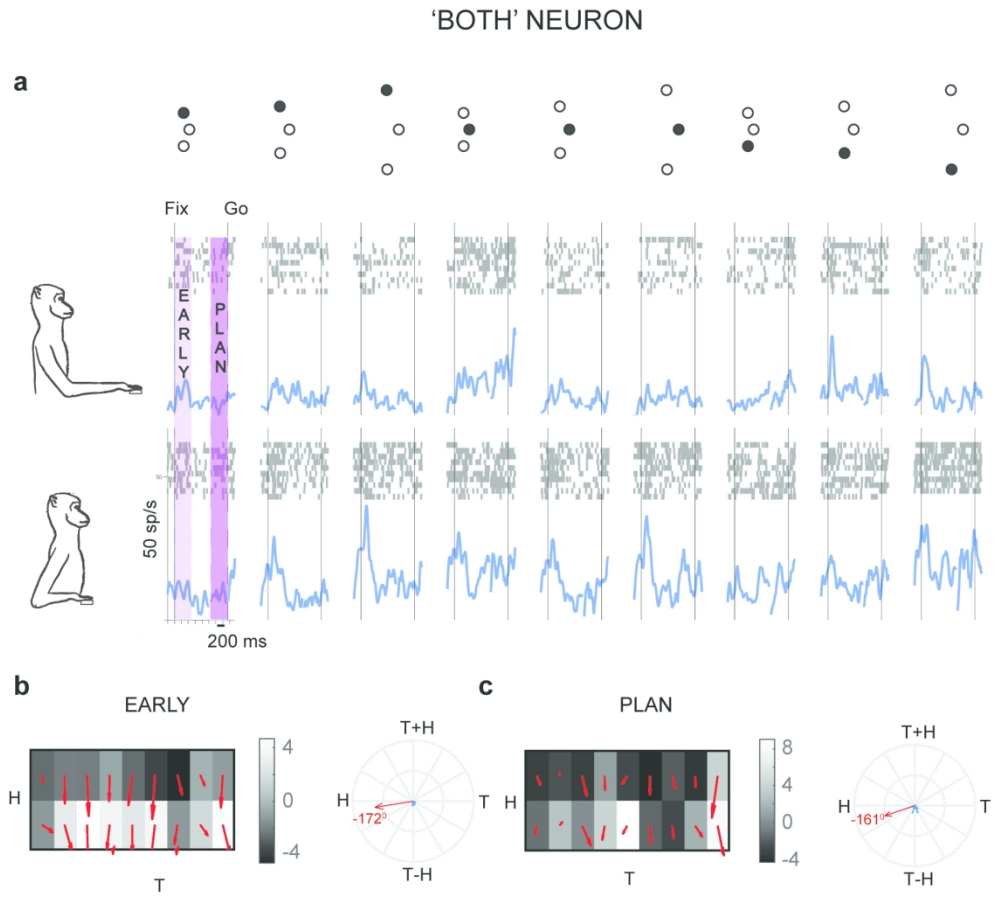

Figure 4

Fig.4. Example neuron showing tuning in both EARLY and PLAN epoch. All figure conventions were as in Fig.3.

155x147mm (300 x 300 DPI)

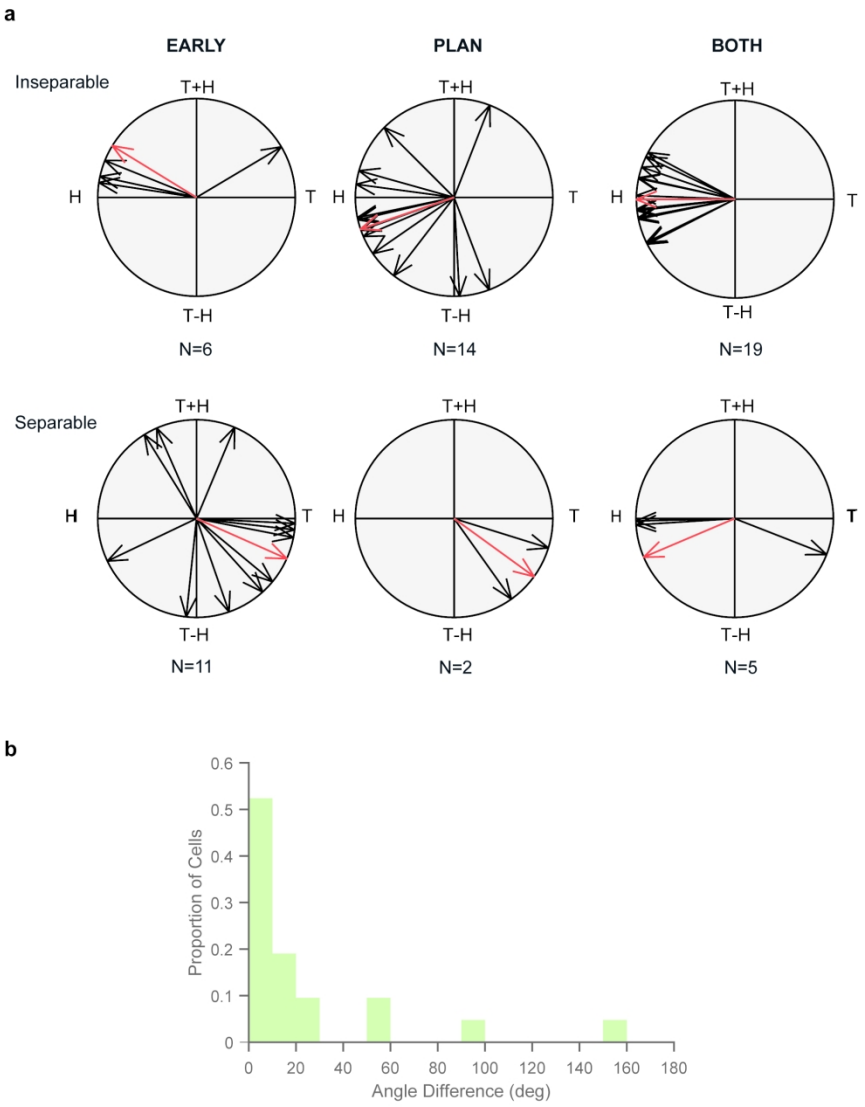

Figure 5

Fig.5. Resultant angle vectors for all the tuned cells (n=56) in the EARLY and/or PLAN epochs.
a. Numbers indicate the number of neurons in each plot, with the number of best tuned neurons in parentheses. Red vectors represent the mean of the black vectors in each plot. In BOTH cells the orientation during PLAN epoch is shown. Please note that in some cases several neurons had very similar resultant angles (e.g. BOTH inseparable cells thick black arrows below red arrow).
b. Angle difference between resultant angle vectors in the cells tuned in both EARLY and PLAN.

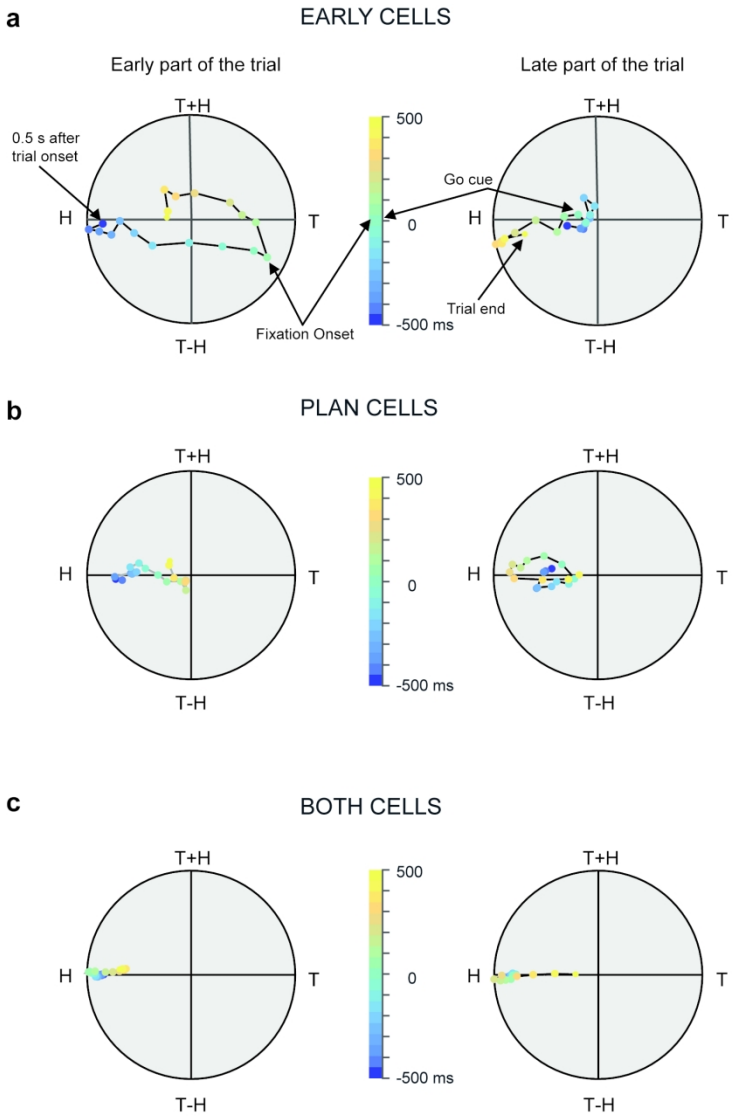

Figure 6

Fig.6. Temporal evolution of reference frames for the population of EARLY-only (a), PLAN-only (b) and both (c) cells active during the fixation-to-hand lift task. In each circular plot, the colored dots represent the average resultant for the each population of cells at 50-ms time steps (300 ms window). The direction of each dot in the circular plot indicates the mean orientation and its distance from the center the strength of tuning. Tuning strength is normalized within each subpopulation and the data were aligned to fixation onset (left plots) and Go cue (right plots).

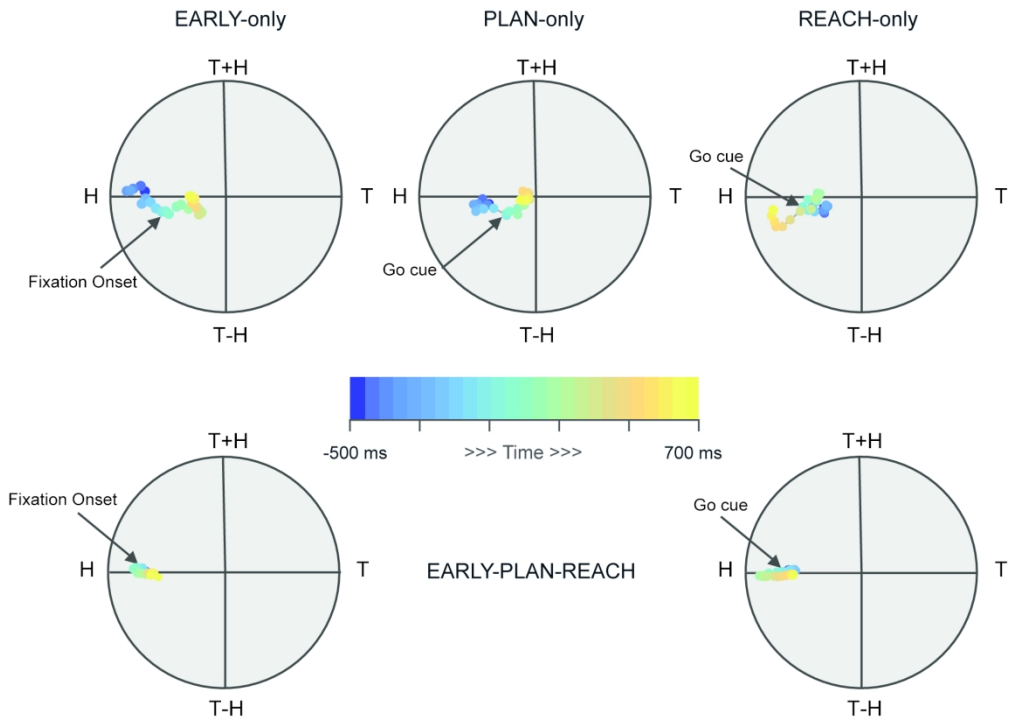

Figure 7

Fig.7. Temporal evolution of reference frames for the main subpopulations of cells active during the fixation-to-reach task. At the top row data were aligned at fixation onset (left) or at the Go cue (middle and right). Same conventions as in Figure 6.

Table 1. Incidence of separable and inseparable tuning in each task and epoch.

Fixate-to-hand lift (n=56/76)

EARLY (n=17)	PLAN (n=15)	BOTH (n=24)
6(5-1)/**11(11-0**)	13(12-1)/**2(2-0)**	16(14-2)/**3(3-0)**

Fixate–to-reach (n=193/240)

EARLY (n=22)	PLAN (n=13)	BOTH (n=10)	
16(10-6)/**6(5-1)**	10(8-2)/**3(1-2)**	8(5-3)/**2(2-0)**	
REACH (n=49)	ALL (n=51)	EARLY- REACH (n=23)	PLAN-REACH (n=25)
37(19-18)/**12(9-3)**	26(16/10)/**7(5-2)**	11(3/8)/**3(1-2)**	12(8-4)/**3(2-1)**

The number of tuned inseparable and tuned separable (in bold) neurons for each epoch and task is reported. **Number pairs in parentheses denote the number of cells in the two animals (A-B)**. Asterisks indicate a statistical difference between the 2 animals. Comparing the relative proportions of separable and inseparable cells in the various subpopulations across tasks showed a significant difference only in the cells tuned in epoch EARLY (two-sample binomial test, $p<0.05$).